# 行政院國家科學委員會專題研究計畫　成果報告

## 具陀螺力矩之主動振動控制系統的渾沌反控制與同步

計畫類別：個別型計畫
計畫編號：NSC93-2218-E-164-001-
執行期間：93 年 08 月 01 日至 94 年 07 月 31 日
執行單位：修平技術學院機械工程系

計畫主持人：陳恒輝

報告類型：精簡報告

處理方式：本計畫可公開查詢

中　華　民　國 94 年 10 月 18 日

# 具陀螺力矩之主動振動控制系統的渾沌反控制與同步

CHAOTIC ANTI-CONTROL AND SYNCHRONIZATION OF ACTIVE VIBRATION CONTROL SYSTEM WITH GYROSCOPIC MOMENT

計畫編號：NSC 93-2218-E164-001
執行期限：93 年 08 月 01 日至 94 年 07 月 31 日
主持人：陳恒輝 副教授 修平技術學院機械工程系
計畫參與人員：黃韋綸 研究生研究助理 大業大學機電自動化研究所

**中文摘要**

本計畫擬以伺服陀螺儀為主動控制元件，對具單擺振動模式之航空器作振動控制。系統架構由單擺、伺服陀螺儀與直流無刷馬達所構成的。伺服陀螺儀為系統的主動控制元件，其陀螺力矩可以作為角度穩定，消振及位置等控制系統的伺服力矩。在單擺系統中伺服陀螺儀為提供消振阻尼力矩的元件，考量其角動量大小方向會隨馬達轉角變化有所改變限制，將陀螺輸出力矩設計為一控制器，對單擺振動系統作振動控制。因系統存在耦合非線性項，對系統非線性動力特性分析是極為重要的，但迄今對其所作的動力分析，多以線性近似方程為基礎，顯然在精確性和可靠性方面存在著問題。本計畫將採用精確拉格朗日非線性運動微分方程，加以作詳細的系統非線性動力與渾沌動力分析，並設計系統控制律。

**關鍵詞**：振動控制、陀螺力、渾沌反控制、渾沌同步

**Abstract**

This project would provide an active vibration control device based on gyroscopic moments to suppress the vibration of the excited pendulum system. The gyroscopic moment induced by a single-gimbal control moment gyroscope is theoretically analyzed, and a controller is derived. An analysis of stability and chaotic dynamics of CMG (control moment gyro) is presented. The necessary and sufficient conditions of stability for the autonomous case were provided by Routh-Hurwitz theory**.** Simulation results with a single-gimbal CMG for a pendulum are carried out. As the electrical time constant is much smaller than the mechanical time constant, the singularly perturbed system can be obtained by the singular perturbation theory. The Liapunov stability of this system by studying the reduced and boundary-layer systems was also analyzed. Using the Melinikov technique, we can give criteria for the existence of chaos in the gyro motion.

Keywords: Vibration Control, Gyroscopic Moment, Chaotic Anti-control, Chaotic Synchronization

## 2.Introduction

In engineering vibratory problems, vibration absorbers are usually to suppress random vibration. However, it is not applicable to suppress the vibration motion for these systems such as the attitude control of spacecraft, the stability of surface vehicles and single rail vehicles and so on, owing to there exists no reaction support. These corresponding vibration systems can suppress by an active vibration control device based on the gyroscopic moment. The CMG (control moment gyro) is also the application of gyroscopic mechanisms that is still studied as an attitude control device for artificial satellites. Various vibration control systems with the CMG have been studied [1-3]. The effectiveness of the gyroscopic moment for both passive and active vibration control was discussed by [1]. The CMG as an active vibration device for the pendulum vibration of a gondola was proposed by [2]. An active vibration control system using a gyro-stabilizer are applied to buildings by [3].

The excited pendulum model is used to model the behavior of many engineering vibration systems, such as offshore platforms, buildings in earthquakes etc. Its study has been widely studied [4-7]. Many complex phenomena of this kind of non-linear dynamic system have been demonstrated. The chaotic pendulum [8-11] is a physically realizable system that exhibits the spectrum of temporal chaotic phenomena, including control [11] and synchronization [12-14]. Synchronization, in particular, has been a recent central focus in chaotic dynamics.

Since Pecora and Carroll proposed their method of synchronizing chaos [12], theoretical as well as experimental research has been carried out in a variety of non-linear dynamic systems. Chaos synchronization makes it possible to synchronize two chaotic systems previously considered impossible. It has widely aroused research including the model of synchronization for chaotic pendulums [13-14].

A theoretical technique, the Melnikov method, is used to give specific criteria for chaotic vibrations. This method is based on inspecting the topological behavior of horseshoe maps and homoclinic orbits associated to hyperbolic saddle points in phase space. Melnikov analysis is applied to a generalized perturbed pendulum system by Trueba [15], with the result of general formula for the appearance of chaotic motions that incorporate several particular cases. Wiggins and Holmes [16] develop perturbation methods based on the ideas of Melnikov for slowly varying oscillators in three-dimensional space. The details of Melnikov's method can be found in Refs. [15-17]

This project would provide a vibration control device based on the control moment gyro to suppress the vibration of the excited pendulum system. The coupled system is composed of the pendulum, control moment gyro and DC motor. The CMG is the main component of the active vibration control device as a damping mechanism. It turns out that the effect of gyroscopic moment depends on the rotating speed of the gyroscope. The gyroscopic moment of the CMG induced by its gimbal rotation directly controlled by an electric motor. In gyroscopic systems, the dynamics of gyros also exhibit chaotic behavior. It will exhibit nonlinear phenomena including the existence of periodic, quasi-periodic and chaotic motions of the system. The stability conditions and degeneracy surfaces of the system were derived by Routh-Hurwitz theory. When the time constant of controller is much smaller than the mechanical one the singularly perturbed system can be obtained by singular perturbation theory. The Liapunov stability of the reduced and boundary-layer systems are also analyzed. As the reduced system is subjected to the periodic perturbation, a version of Melnikov method is used to obtain criteria for the existence of chaotic motion.

## 3. Equations of Motion

The coupled system is composed of the pendulum, control moment gyro and brushless DC motor as shown in Fig. 1. The CMG (control moment gyro) is the main component of the active vibration control device as a damping mechanism as shown in Fig. 2. It turns out that the effect of gyroscopic moment depends on the rotating speed of the gyroscope. The gimbal movement of CMG is directly controlled with BLDC motor, thus it can be used as a sliding controller. The gimbal angle is denoted as $\theta$.

3.1 Gyro System

The gimbals can turn about output X-axis with rotational angle $\theta$. Motion about this axis is resisted by the torsional spring and damping torque defined by $K_S\theta$, $C_d\dot{\theta}$, respectively. Using Largrange's equation, the differential equation for the output deflection angle $\theta$ of a rate gyro with feedback control is derived as follows:

$$(A+A_g)\ddot{\theta}+C_d\dot{\theta}+K_S\theta+Cn_R(\omega_Y\cos\theta+\omega_Z\sin\theta)+(A+B_g-C_g)[1/2(\omega_Y^2-\omega_Z^2)\sin2\theta-\omega_Y\omega_Z\cos2\theta)+(A+A_g)\dot{\omega}_X=T_c, \tag{1}$$

where

$$Cn_R = C(\dot{\psi}-\omega_Y\sin\theta+\omega_Z\cos\theta)=const..$$

$\omega_X$, $\omega_Y$ and $\omega_Z$ denote the angular velocity components of the platform along output axis X, input axis Y, and normal axis Z, respectively. *A*, *A* (=*B*), *C* and $A_g, B_g, C_g$ denote the moments of inertia of rotor and gimbals for the gimbals axes $\xi$, $\eta$, $\zeta$, respectively. In planar motion, $\omega_Y=-\dot{\alpha}, \omega_Z=0$ and $\dot{\omega}_X=0$, Eq. (1) becomes

$$(A+A_g)\ddot{\theta}+C_d\dot{\theta}+K_S\theta-Cn_R\dot{\alpha}\cos\theta+1/2(A+B_g-C_g)\dot{\alpha}^2\sin2\theta=T_c \tag{2}$$

The output torque around the *Y*-axis is $T_Y=Cn_R\dot{\theta}\cos\theta$, and around the axis perpendicular to both *X* and *Y*, $T_Z=Cn_R\dot{\theta}\sin\theta$ $\dot{\omega}_X=T(I,\theta)$. When the gimbal movement is negligible small, the output torque around the Y-axis is proportional to $\dot{\theta}$. $T_c$ is the control-motor torque along the output axis of the system to balance the corresponding gyroscopic torque. The torque and electric current of control-motor can be modeled by the following relation:

$$T_c=K_TI, \tag{3}$$

$$L\dot{I}+RI=K_a(\theta_d-\theta)-K_0\dot{\theta}, \tag{4}$$

where electromotive force is proportional to the difference between the prescribed motion $\theta_d(t)$ and the rotational angle $\theta$, that is $v=K_a(\theta_d-\theta)$. It is applied to the control-motor. *I, R, L*, and $K_0$ are the current, resistance, inductance, and back-electromotive constant of the control-motor; $K_T$ denotes the torque constant of the control-motor.

3.2 Active Vibration Control system

The equation of motion of the active vibration is given as

$$J_p\ddot{\alpha}+C_{pd}\dot{\alpha}+m_pgl\sin\alpha=u, \tag{5}$$

where $\alpha$ is the swing angle of the pendulum, $J_P$ is the inertia moment, $C_{Pd}$ is damping torque, $m_P$ is the mass, $l$ is the arm length, $g$ is the gravity acceleration and *u* is the gyroscopic moment of CMG.

Case 1

In this active control we use CMG as a damping moment, and the relationship of the swing angle velocity $\dot{\alpha}$ and the CMG gimbal angle velocity $\dot{\theta}$ is

expressed as follows

$$u = -T_Y = -Cn_R\dot{\theta}\cos\theta \quad (6)$$

$$\dot{\theta} = K_P\dot{\alpha}, \quad (7)$$

where $K_P$ is the coefficient of the control. So the damping characteristics of the pendulum with CMG can be expressed as

$$\zeta=(K_PCn_R\cos\theta+C_{Pd})/(2J_P\omega_0),\ \ \omega_0=\sqrt{m_Pgl/J_P}=\sqrt{g/l}, \quad (8)$$

where $\zeta$ is the damping ratio of the pendulum with CMG and $\omega_0$ is the angular frequency of the pendulum.

Case 2

The control law is the velocity feedback $u=-K_u\dot{\alpha}$ that applies the gyroscopic torque proportional to the angular speed $\dot{\alpha}$. The damping characteristics of the resulting pendulum with CMG can be expressed as

$$\zeta=(K_u+C_{Pd})/(2J_P\omega_0),\ \ \omega_0=\sqrt{m_Pgl/J_P}=\sqrt{g/l} \quad (9)$$

where $\zeta$ is the damping ratio of the pendulum with CMG and $\omega_0$ is the angular frequency of the pendulum.

In order to avoid saturation for an impulse response solution $\alpha = Ae^{-\zeta\omega_0 t}\sin\omega_0\sqrt{1-\zeta^2}t$, the inequality should be satisfied [1].

$$C|n_R|\sin\theta_{\max} \geq 2J_PA\zeta\sqrt{1-\zeta^2}\omega_0e^{-\zeta\omega_0t_q} \quad (10)$$

where The moment $t=t_q$ is the first time when $\dot{\alpha}=0$, about a quarter period after the beginning, $t=0$. If there is no limit for $\theta$ and $\zeta$ is small, then the equality in Eq. (10) is rewritten as

$$C|n_R| \approx 2J_PA\zeta\omega_0 \quad (11)$$

The damping ratio $\zeta$ is almost proportional to $|n_R|$.

Eq. (6) gives a precise estimation of the output torque to the pendulum. When the gimbal movement is negligibly small, the output torque around Y-axis is proportional to $\dot{\theta}$. Meanwhile the reaction to the gimbal of the CMG is estimated as $-Cn_R\dot{\alpha}\cos\theta$. The gimbal movement should be controlled, preserving the relation Eq. (6) to perform positive work, i.e., to avoid the actuator sometimes acts as a controlled break. Thus, we are interested in the stability of the actuator.

## 4. The stability of gimbal motion

In this section, the stability of gyro system is discussed by distinct methods. When the main pendulum system is steady rotating, the stability of the autonomous system is analyzed to obtain the necessary and sufficient conditions for locally asymptotical stable motion at the fixed point by Routh-Hurwitz criterion. In addition, the Liapunov direct method was used to obtain the conditions sufficient for asymptotical stability and instability of motion of the feedback control system.

For the case when the perturbed angular velocity $\omega_Z = \omega_{ZC} = const.$, the perturbed angular acceleration $\dot{\omega}_X = \dot{\omega}_{X0} = const.$, and the input angular velocity $\omega_Y = 0$, this system is autonomous. One stationary point of the nonlinear autonomous system is the origin ($x$, $y$, $z$)=(0, 0, $z_0$), where $z_0=\dot{\omega}_{X0}/D_2$, $x_d = D_5\dot{\omega}_{X0}/D_2D_6$. Let the disturbed motion be $x=0+x_1$, $y=0+x_2$, $z=z_0+x_3$, so the Eq.s (1-3) for disturbances are as:

$$\begin{aligned}\dot{x}_1 &= x_2,\\ \dot{x}_2 &= -D_1x_2 - Q_Cx_1 + D_2x_3 + O(x_1^2),\\ \dot{x}_3 &= -D_5x_3 - D_6x_1 - D_7x_2,\end{aligned} \quad (12)$$

where $Q_C = D_{2S} + D_3\omega_{ZC} - D_4\omega_{ZC}^2$.

First, the conditions for the stability of the origin of the autonomous system will be obtained by using the Routh-Hurwitz criterion.

The Jacobian matrix ***J*** at the origin of the system (12) is in the form of

$$\boldsymbol{J}=\begin{bmatrix}0 & 1 & 0\\ -Q_C & -D_1 & D_2\\ -D_6 & -D_7 & -D_5\end{bmatrix}. \quad (13)$$

and the characteristic equation of ***J*** in the form of

$$\lambda^3+(D_5+D_1)\lambda^2+(D_2D_7+Q_C+D_1D_5)\lambda$$
$$+(Q_CD_5+D_6D_2)=0 \text{ or } \lambda^3+a_1\lambda^2+a_2\lambda+a_3=0. \quad (14)$$

The Hurwitz matrix ***H*** for the above polynomial is

$$\boldsymbol{H}=\begin{bmatrix}a_1 & 1 & 0\\ a_3 & a_2 & a_1\\ 0 & 0 & a_3\end{bmatrix}. \quad (15)$$

The necessary and sufficient conditions for all the roots of characteristic Eq. (14) to have negative real parts are provided by the Routh-Hurwitz criterion, i.e., the principle minors of the Hurwitz matrix ***H*** must all be positive. So, the stability conditions are obtained as follows

$$D_5+D_1>0 \quad (16.a)$$

$$D_5D_2D_7+D_1D_5^2+D_1D_2D_7+D_1Q_C+D_1^2D_5-D_6D_2>0,$$

i.e., $e_1\omega_{ZC}^2+e_2\omega_{ZC}+e_3<0$, (16.b)

$$Q_CD_5+D_6D_2>0, \text{ i.e., } e_4\omega_{ZC}^2+e_5\omega_{ZC}+e_6<0, \quad (16.c)$$

where $e_1=e_4=D_4>0$, $e_2=e_5=-D_3$, $e_3=-D_{2S}-(D_5D_2D_7+D_1D_5^2+D_1D_2D_7+D_1^2D_5-D_6D_2)/D_1$, $e_6=-D_{2S}-D_6D_2/D_5$.

The above stability conditions can be rewritten as

$$\omega_{ZC1} < \omega_{ZC} < \omega_{ZC2}, \quad (17)$$

According to the Routh-Hurwitz criterion, the necessary and sufficient conditions for stability are as follows

$$\omega_{ZC1} < \omega_{ZC} < \omega_{ZC2}, \quad (18)$$

where $\omega_{ZC1}=(D_3-(D_3^2+4D_4(D_{2S}+p_{\min}))^{1/2})/(2D_4)$,

$\omega_{ZC2}=(D_3+(D_3^2+4D_4(D_{2S}+p_{\min}))^{1/2})/(2D_4)$,
$p_{\min}=Min(e_3^*,e_6^*)$,$e_3^*=(D_5D_2D_7+D_1D_5^2+D_1D_2D_7+D_1^2D_5-D_6D_2)/D_1$, $e_6^*=D_6D_2/D_5$.

That all the roots of the characteristic polynomial of the Jacobian matrix ***J*** have negative real parts, i.e., the motion of the linearized autonomous system is asymptotically stable at the fixed point. Alternatively, the system possesses critical behavior when Jacobian matrix ***J*** contains eigenvalues with zero real parts in the following degeneracy surfaces:

1. There exists one zero eigenvalue ($\lambda_1=0$) of this linearized system for the system parameter $Q_C=-D_6D_2/D_5$, i.e., $\omega_{ZC}=\omega_{ZC1}$ or $\omega_{ZC2}$, on stability boundary, $p_{\min}=e_6^*$. The residual eigenvalues are $\lambda_{2,3}=\{-(D_1+D_5)\pm[(D_1+D_5)^2-4(D_2D_7-D_6D_2/D_5+D_1D_5)]^{1/2}\}/2$;
2. There exists a pair of pure imaginary eigenvalues ($\lambda_{1,2}=\pm j\omega_0$) of this linearized system for the system parameter $Q_C=-(D_5D_2D_7+D_1D_5^2+D_1D_2D_7+D_1^2D_5-D_6D_2)/D_1$, i.e., $\omega_{ZC}=\omega_{ZC1}$ or $\omega_{ZC}=\omega_{ZC2}$, $p_{\min}=e_3^*$, where $\omega_0=(-D_1(D_5D_2D_7+D_1D_5^2-D_6D_2))^{1/2}/D_1$ is a real number, i.e., $D_2>D_1D_5^2/(D_6-D_5D_7)$. The residual eigenvalue is $-(D_1+D_5)$;
3. There exists a double zero eigenvalues ($\lambda_{1,2}=0,0$) for (a) the system parameter $Q_C=-D_1D_5D_6/(D_6-D_5D_7)$ and $D_2=D_1D_5^2/(D_6-D_5D_7)$, the residual eigenvalue is $-(D_1+D_5)$; (b) the system parameter $Q_C=-D_6D_2/D_5$ and $D_1=D_2(D_6-D_5D_7)/D_5^2$, the residual eigenvalue is still in the form of $-(D_1+D_5)$ but the value adapts for varying the system parameter $D_1$.

## 5. Singular perturbation model

To facilitate the analysis, in the interest of model simplification, we usually neglect those small physical parameters to reduce orders of a model. Singular perturbations are used to simplify the model and to provide tools for improving oversimplified models when the original full order model satisfies the some assumptions. To obtain the standard singular perturbation model, let us define the variables $p_1=x$, $p_{1d}=x_d$, $p_2=T_m y$, $q=(T_m^2D_2)z$, $t=T_m\tau$, $T_m=D_5/(D_1D_5+D_2D_7)$, $T_e=1/D_5$, $\varepsilon=T_e/T_m$, and rewrite the state Eq. (4) as

$$
\begin{aligned}
&p_1'=p_2,\\
&p_2'=-a_1p_2-(a_{2S}p_1+a_3\tilde{\omega}_Z\sin p_1+1/2a_4(\tilde{\omega}_Y^2-\tilde{\omega}_Z^2)\sin 2p_1)\\
&-(a_3\tilde{\omega}_Y\cos p_1-a_4\tilde{\omega}_Y\tilde{\omega}_Z\cos 2p_1+\tilde{\omega}_X')+q,\\
&\varepsilon q'=-q+a_5(p_{1d}-p_1)-a_6p_2,
\end{aligned}
\tag{19}
$$

or in the compact form $\dot{p}=f_0(t,p,q,\varepsilon)$, $\varepsilon\dot{q}=g_0(t,p,q,\varepsilon)$, where $p=[p_1,p_2]$, $f_0=[f_{01},f_{02}]$, $a_1=D_1T_m$, $a_{2S}=D_{2S}T_m^2$, $a_3=D_3T_m^2$, $a_4=D_4T_m^2$, $a_5=D_2D_6T_m^2/D_5$, $a_6=D_2D_7T_m/D_5$, $\tilde{\omega}_Y(\tau)=\omega_Y(T_m\tau)$, $\tilde{\omega}_Z(\tau)=\omega_Z(T_m\tau)$, $\tilde{\omega}_X'(\tau)=T_m\omega_X'(T_m\tau)$.

We assume that $\varepsilon<<1$. This assumption means that the mechanical time constant $T_m$ is sufficiently larger than the electrical time constant $T_e$. By using the singular perturbation theory to consider the singularly perturbed system (19), at $\varepsilon=0$, the slow manifold is

$$q=h(\tau,p)=-a_5(p_1-p_{1d})-a_6p_2.$$

The corresponding slow model, $p'=f_0(\tau,p,h(\tau,p),0)$,

$$
\begin{aligned}
&p_1'=p_2,\\
&p_2'=-M(p_1,\tilde{\omega}_Z,\tilde{\omega}_Y)-N(p_2)+(a_5p_{1d}-\tilde{\omega}_X'),
\end{aligned}
\tag{20}
$$

where

$$
\begin{aligned}
M(p_1,\tilde{\omega}_Z,\tilde{\omega}_Y)&=(a_{2S}+a_5)p_1+a_3\tilde{\omega}_Z\sin p_1\\
&+1/2a_4(\tilde{\omega}_Y^2-\tilde{\omega}_Z^2)\sin 2p_1+(a_3\tilde{\omega}_Y\cos p_1-a_4\tilde{\omega}_Y\tilde{\omega}_Z\cos 2p_1)
\end{aligned}
$$

$N(p_2)=(a_1+a_6)p_2$.

For the case when $\tilde{\omega}_X'=\tilde{\omega}_{X0}'=const.$, $\tilde{\omega}_Z=\tilde{\omega}_{ZC}=const.$, and $\tilde{\omega}_Y=0$, the system has one isolated equilibrium point at the origin where $p_{1d}=\tilde{\omega}_{X0}'/a_5$. Depending unpon the functions $M(\cdot)$ and $N(\cdot)$ it might have other equilibrium points. A Lyapunov function candidcate may be taken as the energy-like function

$$V(p)=\int_0^{p1}M(y,\tilde{\omega}_{ZC},0)dy+1/2\,p_2^2. \tag{21}$$

The derivative of $V(p)$ along the trajectories of the system is given by

$$V'(p)=-p_2N(p_2)\le 0. \tag{22}$$

Thus, $V'(p)$ is negative semidefinite. According to the theorems of Barbashin and Krasovskii, the only solution of the system that can stay in $S=\{p\in\Re^2\mid p_2=0\}$ for all $\tau$ is the trivial solution $p(\tau)=0$ if $M(0,\tilde{\omega}_{ZC},0)=0$, $p_1M(p_1,\tilde{\omega}_{ZC},0)>0$ for $p_1\neq 0$ is satisfied , i.e.,

$$
\begin{aligned}
p_1M(p_1,\tilde{\omega}_{ZC},0)&=p_1((a_{2S}+a_5)p_1+a_3\tilde{\omega}_{ZC}\sin p_1-a_4\tilde{\omega}_{ZC}^2\cos p_1\sin p_1)\\
&>p_1((a_{2S}+a_5)\sin p_1+a_3\tilde{\omega}_{ZC}\sin p_1-a_4\tilde{\omega}_{ZC}^2\sin p_1)>0
\end{aligned}
\tag{23}
$$

when the following condition is held:

$$\tilde{\omega}_{ZC1}<\tilde{\omega}_{ZC}<\tilde{\omega}_{ZC2} \tag{24}$$

where

$$
\begin{aligned}
\tilde{\omega}_{ZC1}&=(a_3-\sqrt{a_3^2+4(a_{2S}+a_5)a_4})/(2a_4)\\
&=(D_3-\sqrt{D_3^2+4D_4[D_{2S}+D_2(D_6/D_5)]})/(2D_4),\\
\tilde{\omega}_{ZC2}&=(a_3+\sqrt{a_3^2+4(a_{2S}+a_5)a_4})/(2a_4)\\
&=(D_3+\sqrt{D_3^2+4D_4[D_{2S}+D_2(D_6/D_5)]})/(2D_4)
\end{aligned}
.
$$

Thus, the origin is asymptotically stable.

For the case when $\tilde{\omega}_Y$ , $\tilde{\omega}'_X$ and $\tilde{\omega}_Z$ are time-varying function, the system has an exponentially stable motion $(p_1, p_1') = (p_{10}(\tau), p'_{10}(\tau))$ where $p_{1d} = 0$ , when the following condition is held:

$$\tilde{\omega}_{Z1} < \tilde{\omega}_Z(\tau) < \tilde{\omega}_{Z2} \tag{25}$$

where

$$\tilde{\omega}_{Z1} = (a_{3\tau} - \sqrt{a_{3\tau}^2 + 4(a_{2S}^* + a_5)a_{4\tau}})/(2a_{4\tau})$$
$$= (D_{3t} - \sqrt{D_{3t}^2 + 4D_{4t}[D_{2S}^* + D_2(D_6/D_5)]})/(2D_{4t})$$
$$\tilde{\omega}_{Z2} = (a_{3\tau} + \sqrt{a_{3\tau}^2 + 4(a_{2S}^* + a_5)a_{4\tau}})/(2a_{4\tau})$$
$$= (D_{3t} + \sqrt{D_{3t}^2 + 4D_{4t}[D_{2S}^* + D_2(D_6/D_5)]})/(2D_{4t})$$

and $a_{4\tau} > 0$, i.e., $-\pi/4 < p_{10} < \pi/4$, $a_{3\tau}=a_3\cos(p_{10})$, $a_{4\tau}=a_4\cos(2p_{10})$, $a_{2S}^* = a_{2S} + a_{4t}\omega_Y^2$, i.e., $D_{4t} > 0$, $-\pi/4 < \theta_0 < \pi/4$, $D_{3t}=D_3\cos(\theta_0)$, $D_{4t}=D_4\cos(2\theta_0)$, $D_{2S}^* = D_{2S} + D_{4t}\omega_Y^2$,

which can be derived by the same form of Liapunov functions as reference. The origin of the corresponding boundary-layer system

$$\frac{d\gamma}{d\tau} = g_0(\tau, p, \gamma + h(\tau, p), 0) = -\gamma \tag{26}$$

is exponentially stable uniformly in ($\tau$, $p$). Since $f_0$ and $g_0$ of Eq. (19) also satisfy the conditions of Appendix I, we conclude that the origin of the full singularly perturbed system (34) is exponentially stable for sufficiently small . Thus, the necessary and sufficient condition for asymptotic stability is the Eq. (25).

In Section 4, a three-dimensional dynamic system is considered. In Section 5, we consider the case in which the mechanical time constant is sufficiently larger than the electrical time constant. Thus the system can be reduced to a two-dimensional system by singular perturbations which simply the order of the model and provide tools for improving oversimplified models.

## 6. The Melnikov analysis

In previous studies, both complete nonlinear and full singularly perturbed models are considered by the Liapunov direct method and singular perturbation theory respectively. The stability of a single-axis rate gyro mounted in a space vehicle that is spinning with uncertain angular velocity $\omega_Z(t)$ about the spin axis of the gyro is established. In this section, we further study the chaotic dynamics of the reduced system as Eq. (35), where $p_{1d}$=0, when the vehicle undergoes perturbed harmonic rotation about X-axis, and harmonic rotation concerning Z-axis, i.e., $\tilde{\omega}_Y = 0$, $\tilde{\omega}_Z = \tilde{\omega}_{ZC} + \nu_1\cos(\omega_1\tau + \delta_1)$, $\tilde{\omega}_X = \tilde{\omega}_{XC} + \nu_2\sin(\omega_2\tau + \delta_2)$ , $\tilde{\omega}'_X = \frac{d}{d\tau}\tilde{\omega}_X = \nu_2\omega_2\cos(\omega_2\tau + \delta_2)$ ; $\nu_i$ and $\omega_i$ are the amplitude and frequency of the perturbed angular velocity of vehicle.

Here, we assume that the angular velocity of vehicle is of small disturbance near a constant angular velocity, i.e., $\tilde{\omega}_{ZC} = const.$ , $\varepsilon\bar{\nu}_1 = \nu_1$ and $a_3\omega_0 >> 1$ . Changing time variable $\bar{t} = \omega_n\tau$ , $\omega_n^2 = a_3\tilde{\omega}_{ZC}$ and letting $q_1 = p_1, q_2 = \dot{q}_1$, $\varepsilon b_1 = (a_1 + a_6)/\omega_n$, $\varepsilon b_2 = (a_{2S} + a_5)/\omega_n^2$, $\varepsilon b_3 = -(a_4\tilde{\omega}_{ZC}^2/2 + a_4\nu_1^2/4)/\omega_n^2$ , $\varepsilon b_4 = \nu_1 a_3/\omega_n^2$ , $\varepsilon^2 b_5 = -\nu_1 a_4\tilde{\omega}_{ZC}/\omega_n^2$ , $\varepsilon^2 b_6 = -\nu_1^2 a_4/\omega_n^2$ , $\varepsilon b_7 = -\nu_2\Omega_2/\omega_n$, $\Omega_1 = \omega_1/\omega_n$, $\Omega_2 = \omega_2/\omega_n$.

In Eq. (20), we have the perturbation form $\dot{q}_1 = q_2$,

$$\dot{q}_2 = -\sin q_1 + \varepsilon(-b_1 q_2 - b_2 q_1 - b_3\sin 2q_1 - b_4\sin q_1\cos(\Omega_1\bar{t} + \delta_1) - b_5\sin 2q_1\cos(\Omega_1\bar{t} + \delta_1) - b_6\sin 2q_1\cos 2(\Omega_1\bar{t} + \delta_1) - b_7\cos(\Omega_2\bar{t} + \delta_2)) \tag{27}$$

in the compact form

$$\dot{q} = f(q) + \varepsilon g(q, \bar{t}) \tag{28}$$

where

$$q = [q_1, q_2], f(q) = [f_1(q), f_2(q)], g(q, \bar{t}) = [g_1(q, \bar{t}), g_2(q, \bar{t})].$$

For $\varepsilon = 0$, the system (28), which has centers at (0, 0) and hyperbolic saddles at $q_0^{\pm} = (\pm\pi, 0)$ , is a Hamiltonian system with a Hamiltonian function

$$H(q_1, q_2) = \frac{1}{2}q_2^2 - \cos(q_1). \tag{29}$$

The Hamiltonian system has homoclinic orbits that connect different saddle points $q_0^{\pm}$ . Hence the hyperbolic periodic orbits of the Hamiltonian system, for $H(q_1, q_2) = h = 1$, are given by

$$q_h^{\pm}(t) = (q_{1h}^{\pm}, q_{2h}^{\pm}) = (\pm 2\tan^{-}\sinh t, \pm 2\operatorname{sech} t) \tag{30}$$

We will compute the Melnikov function for $q_h^+$ (the computation for $q_h^-$ is identical).

The Melnikov function is given by [16]

$$M^+(t_0) = \int_{-\infty}^{\infty} f(q_h^+(\bar{t}))\wedge g(q_h^+(\bar{t}), \bar{t} + \bar{t}_0)d\bar{t} = -M_1^+ - M_2^+ - M_3^+ - M_4^+ - M_5^+ \tag{31}$$

where

$$f(q_h^+(\bar{t})) = q_{2h}^+(\bar{t}),$$
$$g(q_h^+(\bar{t}), \bar{t} + \bar{t}_0) = -b_1 q_{2h}^+(\bar{t}) - b_2 q_{1h}^+(\bar{t}) - b_3\sin 2q_{1h}^+ - b_4\sin q_{1h}^+(\bar{t})\cos(\Omega_1(\bar{t} + \bar{t}_0) + \delta_1) - b_7\cos(\Omega_2(\bar{t} + \bar{t}_0) + \delta_2)$$

$$M_1^+ = b_1\int_{-\infty}^{\infty} q_{2h}^+(\bar{t})q_{2h}^+(\bar{t})d\bar{t} = b_1\int_{-\infty}^{\infty}(2\operatorname{sech}\bar{t})^2 d\bar{t} = 8b_1 \tag{32.a}$$

$$M_2^+ = b_2\int_{-\infty}^{\infty} q_{2h}^+(\bar{t})q_{1h}^+(\bar{t})d\bar{t} = b_2\int_{-\infty}^{\infty}(2\operatorname{sech}\bar{t})(2\tan^{-}(\sinh\bar{t}))d\bar{t} = 0 \tag{32.b}$$

$$M_3^+ = b_3\int_{-\infty}^{\infty} q_{2h}^+(\bar{t})\sin 2(q_{1h}^+(\bar{t}))d\bar{t} = b_3\int_{-\infty}^{\infty}(2\operatorname{sech}\bar{t})\sin 2(2\tan^{-}(\sinh\bar{t}))d\bar{t} = 0 \tag{32.c}$$

$$M_4^+ = b_4\int_{-\infty}^{\infty} q_{2h}^+(\bar{t})\sin(q_{1h}^+(\bar{t}))\cos(\Omega_1(\bar{t}+\bar{t}_0)+\delta_1)d\bar{t}$$
$$= b_4\int_{-\infty}^{\infty}(2\operatorname{sech}\bar{t})\sin(2\tan^{-}(\sinh\bar{t}))\cos(\Omega_1(\bar{t}+\bar{t}_0)+\delta_1)d\bar{t} \quad (32.d)$$
$$= b_4[-2\pi\Omega_1^2\operatorname{csch}(\frac{\pi\Omega_1}{2})\sin(\Omega_1\bar{t}_0+\delta_1)]$$

$$M_5^+ = b_7\int_{-\infty}^{\infty} q_{2h}^+(\bar{t})\cos(\Omega_2(\bar{t}+\bar{t}_0)+\delta_1)d\bar{t}$$
$$= b_7\int_{-\infty}^{\infty}(2\operatorname{sech}\bar{t})\cos(\Omega_2(\bar{t}+\bar{t}_0)+\delta_1)d\bar{t}\,. \quad (32.e)$$
$$= b_7[2\pi\operatorname{sech}(\frac{\pi\Omega_2}{2})\cos(\Omega_2\bar{t}_0+\delta_2)]$$

The integral $M_4^+$ and $M_5^+$ can be evaluated by the method of residues. Hence, the Melnikov function becomes

$$M^+(t_0) = -M_1^+ - M_2^+ - M_3^+ - M_4^+ - M_5^+$$
$$= -8b_1 - b_4[-2\pi\Omega_1^2\operatorname{csch}(\frac{\pi\Omega_1}{2})\sin(\Omega_1\bar{t}_0+\delta_1)] \quad (33)$$
$$- b_7[2\pi\operatorname{sech}(\frac{\pi\Omega_2}{2})\cos(\Omega_2\bar{t}_0+\delta_2)]$$

Suppose that $M^+(\bar{t}_0)$ has a simple zero, i.e., there exists a point $\bar{t}_0 = \tilde{t}_0$ such that

$$M^+(\tilde{t}_0) = 0,\ \frac{\partial M^+}{\partial \bar{t}_0}(\tilde{t}_0) \neq 0\,,$$

That is

$$\varepsilon M^+(\tilde{t}_0) = \varepsilon b_4 E(\Omega_1) - \varepsilon b_7 R(\Omega_2) - 8\varepsilon b_1 = 0\,, \quad (34)$$

where

$$\varepsilon b_1 = (a_1+a_6)/\omega_n \quad , \quad \varepsilon b_4 = \nu_1 a_3/\omega_n^2 \quad ,$$
$$\varepsilon b_7 = -\nu_2\Omega_2/\omega_n\,,$$

$$E(\Omega_1) = 2\pi\Omega_1^2\operatorname{csch}(\frac{\pi\Omega_1}{2})\sin(\Omega_1\bar{t}_0+\delta_1) \quad ,$$

$$R(\Omega_2) = 2\pi\operatorname{sech}(\frac{\pi\Omega_2}{2})\cos(\Omega_2\bar{t}_0+\delta_2)\,.$$

Then the stable and unstable perturbed manifolds that are close to homoclinic manifolds of the unperturbed system intersect transversely and there exist transverse homoclinic orbits. This implies that chaotic dynamics may occur through the Smale-Birkhoff homoclinic theorem.

The first case that we are interested approaching in here is the case when $\Omega_2 \to 0$, i.e., $\tilde{\omega}_X' = 0$, the vehicle undergoes steady rotation about *X* axis and harmonic rotation concerning Z-axis. For simplicity the initial time is chosen in such a way that the initial phase is $\delta_1 = 0$. For this particular case, the critical forcing amplitude $\nu_{1c}$ is given by

$$\nu_{1c} = \frac{4(a_1+a_6)\omega_n}{a_3\pi\Omega_1^2}\sinh(\frac{\pi\Omega_1}{2}) \quad (35)$$

Another interesting result appears when we consider that the vehicle undergoes high frequency oscillation about *X* and the effect of harmonic rotation concerning Z-axis can be neglected. For simplicity the initial time is chosen in such a way that the initial phase is $\delta_2 = 0$. For this particular case, the critical forcing amplitude $\nu_{2c}$ is given by

$$\nu_{2c} = \frac{4(a_1+a_6)}{\pi\Omega_2}\cosh(\frac{\pi\Omega_2}{2}) \quad (36)$$

Now we consider the case when the vehicle undergoes harmonically in both *X*-axis and Z-axis. In this case, $\nu_1 = \nu_2, \Omega_1 = \Omega_2$, *and* $\delta_1 - \delta_2 = \pi/2$, the critical forcing amplitude $\nu_{1c}$ is given by

$$\nu_{1c} = \nu_{2c} = [4(a_1+a_6)/\pi]$$
$$/[(a_3/\omega_n)\Omega_1^2\operatorname{csc}h(\pi\Omega_1/2) + \Omega_1\operatorname{sec}h(\pi\Omega_1/2)] \quad (37)$$

It follows from the Melnikov theory that if the forcing amplitude $\nu > \nu_{1c}$ *or* $\nu_{2c}$ for a given $\Omega_1$ or $\Omega_2$ the manifolds of the Eq. (27) intersect and may yield horseshoe maps near the saddle points. The critical forcing amplitude was numerically computed and the result is shown in following section.

## 7. Numerical demonstrations

In this section, examples are carried out to examine the various forms of dynamic behavior of the system for the previous analyses by numerical simulation techniques. The parameters of the cases are shown in the Appendix II.

To have a visual information in Eq. (35), we have plotted in Fig. 3. The case shown corresponds to a rate gyro mounted on a space vehicle that undergoes steady rotation about *X*-axis and harmonic rotation concerning Z-axis. The critical forcing amplitude $\nu_{1c}$ increases as the constant angular velocity $\tilde{\omega}_{ZC}$ increases. The presence of a local minimum of the curves, in Fig.3, means that the system is easier in the onset of homoclinic chaos depending on the perturbed angular velocity $\tilde{\omega}_{ZC}$. Also, the onset of homoclinic chaos appears easier when the frequency $\Omega_1$ approaches to the neighborhood of the natural frequency $\Omega_0=1$, for some given $\tilde{\omega}_{ZC}$. In Fig. 4, a plot of the critical forcing amplitude $\nu_{2c}$ versus the frequency $\Omega_2$ is presented. The vehicle undergoes high frequency oscillation about *X* and the effect of harmonic rotation concerning Z-axis can be neglected, i.e., the critical forcing amplitude $\nu_{2c}$ is unconcerned with $\tilde{\omega}_{ZC}$. The Melnikov analysis gives a lower-bound on chaotic behavior. When the vehicle undergoes harmonically in both *X*-axis and Z-axis, the critical forcing amplitude versus the frequency $\Omega_1$ from Eq. (37) is shown as Fig. 5 for $\tilde{\omega}_{ZC}$ =1000 (—), $\tilde{\omega}_{ZC}$ =1500 (---), $\tilde{\omega}_{ZC}$ =2000 (···) and $\tilde{\omega}_{ZC}$ =2500 (-.). As we have done the same study as in Fig. 5, it is easy to see what is the difference between

these two cases: the critical forcing amplitude $\nu_{1c}$ is lower than in the previous case and the one that minimizes the critical forcing amplitude as the frequency $\Omega_1$ is closely the natural frequency $\Omega_0$=1, for some given $\tilde{\omega}_{ZC}$.

## 8. Conclusions

An analysis is presented to a single-axis rate gyro subjected to linear feedback control when the vehicle is simultaneously spinning with uncertain angular velocity $\omega_Z(t)$ about its spin axis and accelerating $\dot{\omega}_X(t)$ with respect to the output axis of the gyro. By using the Liapunov direct method, the conditions sufficient for stability are given as Eq. (19). Here, the term $D_{4t}\omega_Y^2(t)$ increases the effective torsional spring torque, such that the stability domain of the perturbed angular velocity $\omega_Z(t)$ becomes larger. For the autonomous case in which $\omega_Z$ and $\dot{\omega}_X$ are steady, both stability and degeneracy conditions of the fixed point are derived by the Routh-Hurwitz criterion in section 3. The necessary and sufficient conditions for asymptotic stability are obtained as Eq. (33). In section 4, the electrical time constant is much smaller than the mechanical time constant is assumed. The stability of a full singular perturbed system from the reduced and boundary-layer systems are studied in an autonomous system by the Liapunov direct method for sufficiently small $\varepsilon$. In section 5, we obtain criteria for existence of chaos in the reduced system by applying Melnikov method. Plots of the critical forcing amplitude versus the frequency of the perturbed motion are presented for some specific examples. Its critical forcing amplitude is minimized when the perturbed frequency is near the normalized natural frequency.


## Acknowledgments

The authors are grateful to the National Science Council, Republic of China, for supporting this research under grant NSC-93-2218-E164-001.


## References


1. Osamu NISHIHARA, Hiroshi MATSUHISA and Susumu SATO 1992 *JSME International Journal* Series III **35**, No. 1, "Vibration Damping Mechanisms with Gyroscopic Moment".
2. Hiroshi KANKI, Yoshitsugu NEKOMOTO, Hiroyuki MONOBE, Hironobu OGURA and Kiichi KOBAYASH I994 *JSME International Journal* Series C **37**, No. 1, "Development of CMG Active Vibration Control Device for Gondola"
3. M. Yamada, H. Higashiyama, M. Namiki and Y. Kazao 1997 Control Eng. Practice, Vol. 5, No. 9, pp. 1217-1222. Active vibration control system using a Gyro-Stabilizer.
4. M. J. CLIFFORD and S. R. BISHOP 1994 Journal of Sound and Vibration 172, 572-576. Approximating the escape zone for the parametrically excited pendulum.
5. S. R. BISHOP and M. J. CLIFFORD 1996 Journal of Sound and Vibration 189, 142-147. Zones of chaotic behavior in the parametrically excited pendulum.
6. Mawhin J. The forced pendulum: A paradigm for nonlinear analysis and dynamical systems. Exp Math 1998;6:271-87.
7. Kobes R, Liu J ,Peles S. Analysis of a parametrically driven pendulum. Phys Rev E 2001;63:036219.
8. D'Humieres D, Beasley MR, Huberman BH, Libchaber A. Chaotic states and routes to chaos in the forced pendulum. Phys Rev A 1982;26:3483.
9. R. W. LEVEN, B.POMPE, C. WILKE and B. P. KOCH 1985 Physica D 16, 371-384. Experiments on periodic and chaotic motions of a parametrically forced pendulum.
10. Gwinn EG, Westerveld RM. Intermittent chaos and low-frequency noise in the driven damped pendulum. Phys Rev Lett 1985;54:1613.
11. Starrett J, Tagg R. Control of a chaotic parametrically driven pendulum. Phys Rev Lett 1995;74:1974-7.
12. L. M. PECORA and T. L. CARROLL 1990 Physical Review Letters 64, 821-823, Synchronization in chaotic system.
13. Gregory L. Baker, James A. Blackburn, H.J.T. Smith 1999 Physics Letters A 252 191-197. A stochastic model of synchronization for chaotic pendulums.
14. Y. ZHANG, S.Q. HU ANDG. H. DU 1999 Journal of Sound and Vibration 223(2), 247-254. Chaos synchronization of two parametrically excited pendulums.
15. Trueba J.L., Baltanás J.P. and Sanjuán M.A.F. A generalized perturbed pendulum. Chaos, Solitons and Fractals 2003; 15: 911-924.
16. Wiggins S. and Holmes P. Homoclinic Orbits in Slowly Varying Oscillators. SIAM J. Math. Anal 1987; 18: 612-629.
17. Guckenheimer J. and Holmes P. Nonlinear Oscillations, Dynamical Systems and Bifurcation of Vector Fields. New York: Springer-Verlag; 1986, Chaps. 4-7.


## Appendix I

The stability analysis that describes a procedure for constructing Liapunov functions for full singularly perturbed system as follows:

Consider the singularly perturbed nonautonomous system

$$\dot{x} = f(t,x,z,\varepsilon), \quad \varepsilon\dot{z} = g(t,x,z,\varepsilon)$$

Assume that the following assumptions are satisfied for all $(t,x,\varepsilon) \in [0,\infty) \times B_r \times [0,\varepsilon_0]$

(1) $f(t,0,0,\varepsilon) = 0$ *and* $g(t,0,0,\varepsilon) = 0$.

(2) The equation $0 = g(t,x,z,0)$ has an isolated root $z = h(t,x)$ such that $h(t,x) = 0$.

(3) The functions *f*, *g* and *h* and their partial derivatives up to order 2 are bounded for $z\text{-}h(t,x) \in B_\rho$.

(4) The origin of the reduced system

$\dot{x} = f(t, x, h(t, x), 0)$ is exponentially stable.

(5) The origin of the boundary-layer system $\frac{dy}{d\tau} = g(t, x, y + h(t, x), 0)$ is exponentially uniformly stable in $(t, x)$.

Then there exists $\varepsilon^* > 0$ such that, for all $\varepsilon < \varepsilon^*$, the origin of (I1) is exponentially stable.

**Appendix II**

The values of gyro parameters:

$(A+A_g) = 54 dyne\,cm\cdot s^2, Cn_R = 10.8\times10^4 dyne\,cm\cdot s,$

$C_d = 54 dyne\,cm\cdot rad^{-1}\cdot s, K_S = 54\times10^3 dyne\,cm\cdot rad^{-1},$

$D_1 = \frac{C_d}{(A+A_g)} = 1 rad^{-1}\cdot s^{-1}, D_{2S} = \frac{K_S}{(A+A_g)} = 10^3 A^{-1}\cdot rad^{-2}\cdot s^{-2},$

$D_2 = \frac{K_T}{(A+A_g)} = 10^3 A^{-1}\cdot rad^{-2}\cdot s^{-2}, D_3 = \frac{Cn_R}{(A+A_g)} = 200 s^{-1}, D_4 = \frac{(A+B_g-C_g)}{(A+A_g)} = 1,$

$D_5 = R/L = 25 sec^{-1}, D_6 = K_a/L = 250 A\cdot rad^{-1}\cdot s^{-1}, D_7 = K_b/L = 1 A\cdot rad^{-1}$

$T_e = 1/D_5 = 0.04, \quad T_m = D_5/(D_1D_5 + D_2D_7) = 0.714,$

$a_1 = D_1T_m = 0.714, a_3 = D_3T_m^2 = 1020, a_6 = D_2D_7T_m/D_5 = 0.286,$

$\omega_n = \sqrt{a_3\tilde{\omega}_{ZC}}$ .

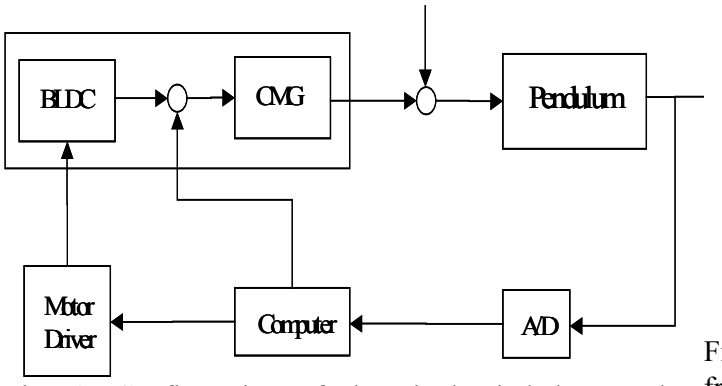


Fig. 1. Configuration of the single-gimbal control moment gyro for the simple pendulum

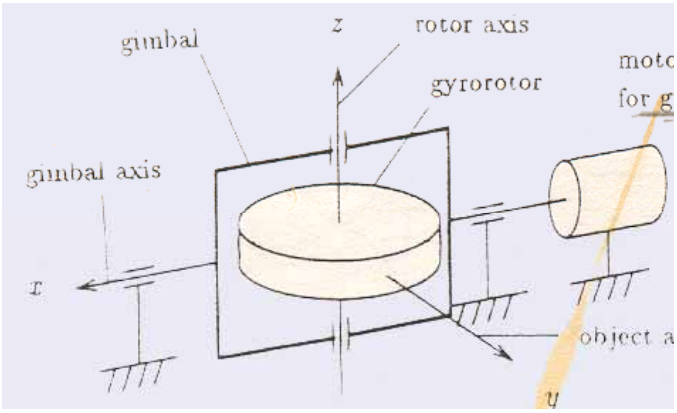


Fig. 2. The single-gimbal control moment gyro

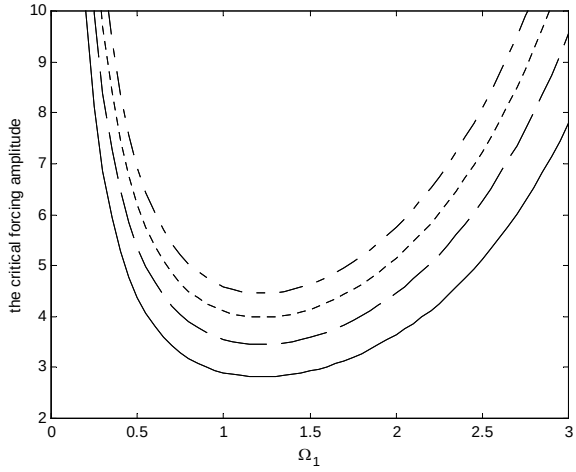


Fig. 3. Plot of the critical forcing amplitude versus the frequency $\Omega_1$ from Eq. (35) for $\tilde{\omega}_{ZC}$ =1000 (—), $\tilde{\omega}_{ZC}$ =1500 (---), $\tilde{\omega}_{ZC}$ =2000 (···) and $\tilde{\omega}_{ZC}$ =2500 (-.).

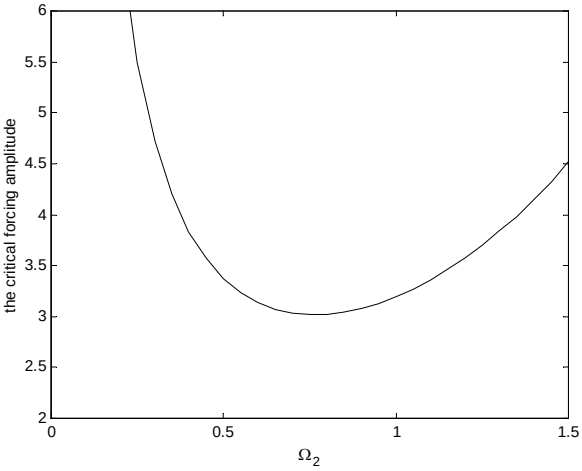


Fig. 4. Plot of the critical forcing amplitude versus the frequency $\Omega_2$ from Eq. (36).

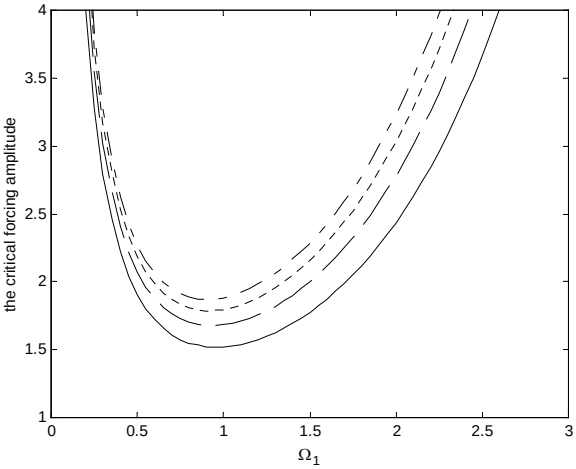


Fig. 5. Plot of the critical forcing amplitude versus the frequency $\Omega_1$ from Eq. (37) for $\tilde{\omega}_{ZC}$ =1000 (—), $\tilde{\omega}_{ZC}$ =1500 (---), $\tilde{\omega}_{ZC}$ =2000 (···) and $\tilde{\omega}_{ZC}$ =2500 (-.).